Journal of
Materials Chemistry A

Accepted Manuscript

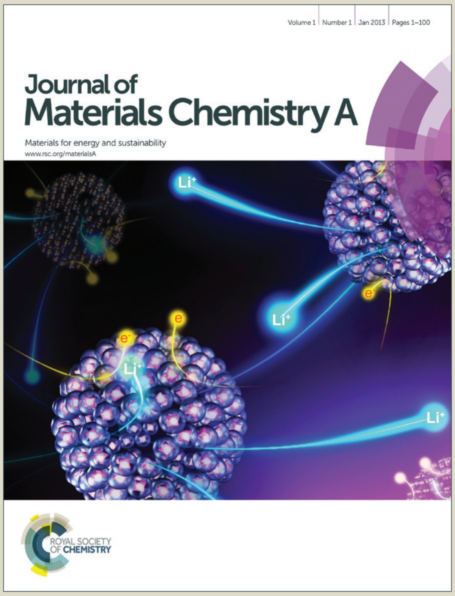

ROYAL SOCIETY
OF CHEMISTRY

www.rsc.org/materialsA

Journal of Materials Chemistry A

Paper

Fabrication of Oleophobic Paper with Tunable Hydrophilicity by Treatment with Non-fluorinated Chemicals

Received 00th January 20xx,
Accepted 00th January 20xx

DOI: 10.1039/x0xx00000x

www.rsc.org/

Zhenguan Tang,[a,b] Dennis W. Hess[a] and Victor Breedveld[a*]

Hydrophilic-oleophobic surfaces have attracted significant attention recently due to their potential use in technologies ranging from oil-water separation to self-cleaning surfaces. However, existing methods rely heavily on fluorinated coating materials, which are harmful to the environment. In this manuscript, a simple, solution based method to fabricate oleophobic paper with tunable hydrophilicity using a non-fluorinated material is reported for the first time. Wetting control is achieved by paper surface modification using a thin film of hydrolyzed methyltrimethoxysilane (MTMS). Hydrophilicity is tuned by adjusting the sonication time during MTMS hydrolysis. ^{29}Si NMR and ATR-FTIR analyses reveal that the change in hydrophilicity is caused by varying the concentration of polar silanol groups in the MTMS solution and, ultimately, on the film surface. The modified paper displays wetting behavior ranging from superhydrophilic/oleophobic (immediate water absorption; motor oil contact angle, 64.2°±1.4°) to amphiphobic (water contact angle 85.2°±3.4°; motor oil contact angle 61.2°±2.5°) as a function of hydrolysis time. For all surface-modified samples, no absorption of motor oil is observed for several weeks, indicating stable oil resistance. Based upon results from SEM, optical profilometry, and air permeability, the intrinsic porosity of paper is also largely retained after coating.

Introduction

Hydrophobic and amphiphobic surfaces have been studied in great depth over the past couple of decades for numerous potential applications.[1-8] Recently, interest has grown in surfaces that simultaneously display a more unusual combination of hydrophilicity and oleophobicity for potential use in industrial applications, like oil/water separation membranes,[9] self-cleaning surfaces[10] and anti-fog surfaces.[11] However, due to the intrinsic difference in surface tension between water and oil, fabrication of such surfaces has proven to be much more challenging than hydrophobic or amphiphobic surfaces.

The wetting behavior of a liquid drop on a smooth, chemically homogeneous surface is governed by Young's equation, which predicts the magnitude of the observed contact angle based on a force balance that includes the solid surface energy, liquid surface tension and adhesive forces at the solid-liquid interface. According to Young's equation, on any given substrate, fluids with lower surface tension will always display smaller contact angles than fluids with higher surface tension; similarly, any specific fluid will wet high-energy surfaces more easily than low-energy surfaces. On chemically homogeneous rough, structured substrates, Young's equation must be modified (e.g. Cassie-Baxter or Wenzel models[12, 13]) but these trends still hold.

Because of the high surface tension of water (~72 mN/m), water-repellent surfaces are easiest to achieve; hydrophobic (static water contact angle WCA > 90°), and even superhydrophobic (WCA > 150°) surfaces or surfaces with tunable hydrophobicity have been successfully developed on a plethora of inorganic and organic materials.[14-21] Because oils generally have a much lower surface tension than water, most hydrophobic substrates are still oleophilic. In order to add oleophobicity and reach amphiphobicity (i.e. oleo- and hydrophobic), it is necessary to combine low surface energy coating materials with carefully engineered surface structures; such properties have been created on various substrates.[22-26]

In order to overcome the limitation that oleophobic substrates are inherently hydrophobic, chemical heterogeneity can be used to introduce favorable interactions with polar liquids, while maintaining unfavorable interactions with nonpolar fluids.[27] Hydrophilic and oleophobic functional groups are generally interspersed along these types of surfaces. Chemical groups with low surface energy contribute to oleophobicity, while polar surface moieties can exhibit sufficiently strong interactions with water molecules to yield hydrophilicity.[28] This concept has been implemented with various coating materials, including polyelectrolyte-fluorinated surfactant complexes,[9, 29, 30] fluorinated polymer brushes,[10, 11, 30-32] fluoroalkylated flip-flop-type silane coupling agents,[33] fluorinated block co-polymers[33] and blends of fluorinated and non-fluorinated polymers.[34]

---

[a] *School of Chemical & Biomolecular Engineering, Georgia Institute of Technology, 311 Ferst Drive NW, Atlanta, Georgia 30332, United States. Email: victor.breedveld@chbe.gatech.edu*

[b] *Renewable Bioproducts Institute, Georgia Institute of Technology, 500 10th Street NW, Atlanta, Georgia 30318, United States*

† Electronic Supplementary Information (ESI) available. See DOI: 10.1039/x0xx00000x

The common characteristic among all existing hydrophilic and oleophobic coating materials is the presence of perfluorinated groups, which are associated with significant environmental and health concerns.[35] Currently, implementation of these materials is also limited by rather complicated coating methods and a fairly low degree of hydrophilicity that leads to slow wetting rates for water.[36] It is therefore desirable to identify alternatives to fluorinated materials for oleophobic/hydrophilic surfaces. One previously identified candidate is methyltrimethoxysilane (MTMS), an organosilane with one methyl group and three hydrolysable methoxy substituents. Taking advantage of the low surface energy properties of methyl side groups,[37] MTMS has been used to impart hydrophobicity and oleophobicity to different substrates such as glass,[38] nanocellulose,[39] wood,[40-42] cotton[43-45] and paper.[46-50] Compared to most fluorinated materials, MTMS has many advantages: lower environmental impact, commercial availability, and compatibility with aqueous processing environments. It is known that hydrolysis is required before MTMS can be chemically bonded to substrates with hydroxyl groups; the impact of this hydrolysis process on the wetting behavior of coated substrates has not been reported.

Another important limitation of prior work is that the majority of hydrophilic/oleophobic surfaces have been fabricated on flat, non-porous surfaces such as silicon wafers,[51] glass slides,[52] and on substrates with well-defined porous structures such as stainless steel meshes[9] and hollow fiber membranes.[53] Creation of hydrophilic and oleophobic properties on substrates with more random structures, such as regular cellulose-based paper, is much less common, in spite of the many practical advantages of paper:[27, 35] low density, low cost, high flexibility, abundance and biodegradability. Paper-based products with selective wetting for oil and water would be highly desirable for cost-effective oil-water separation, for example. Polyelectrolyte-fluorinated surfactant complexes have been previously utilized to create hydrophilic, oleophobic paper,[27] but this method requires a complicated two-step process which inherently limits its wide application in industry and also requires use of fluorinated coating materials.

In this manuscript, a novel one-step method to fabricate paper with tunable wetting properties is reported and the chemical changes that impart such properties are described. By systematically changing the MTMS hydrolysis time prior to coating, different degrees of condensation were achieved, which allowed the paper surface chemistry to be controlled. Paper coated with these different MTMS precursor samples display water wetting behavior ranging from superhydrophilic (absorbs water immediately) to hydrophobic, while oleophobicity is maintained under all conditions. The relation between hydrolysis time, surface chemistry and wetting properties was interrogated using ATR-FTIR, XPS and ^{29}Si NMR, both on flat silicon wafers and on porous paper handsheets. Fluorinated materials are not required in this process, and the intrinsic porosity of paper is largely retained after the coating process based on results from SEM, profilometry and air permeability measurements. The entire coating process is conducted in an aqueous environment under ambient conditions, which renders it compatible with current paper manufacturing processes and offers a scalable, economical and environmentally benign approach to the modification of surfaces.[54-56]

Experimental Section

Handsheet Formation.

For this study, northern bleached softwood Kraft fibers (NBSK) and a mixture of 15% bleached softwood / 85% bleached hardwood fibers (co-pulp) were used to fabricate handsheets; these pulps have already been refined to a consistency of 3.5%. Fabrication of handsheets began by mixing NBSK with the co-pulp in a 40/60 ratio based on dry solids. Handsheets were then formed following TAPPI standardized method T205 sp-02,[57] in which the pulp mixture is lowered in consistency and then drained under gravity through a mesh screen. The wet handsheets were removed from the mesh screen and subsequently pressed at 50 psi. Finally, handsheets were dried overnight under ambient conditions on a stainless steel plate.

MTMS hydrolysis procedure.

Methyltrimethoxysilane (MTMS) was purchased from Sigma-Aldrich (deposition grade, ≥ 98%). Without further purification, MTMS was mixed with 0.1 M hydrochloric acid (HCl, Fisher Chemicals, 37.3%) in a 4:1 v/v ratio. The mixture was then sonicated in an ice-bath for different lengths of time to induce hydrolysis.[50] Sonication was carried out using a Fisher Scientific ultrasonic cleaner (model FS20) at a power of 70 W and frequency of 42 kHz.

MTMS coating procedure.

Silicon wafers (P type 100 mm silicon wafer (100) P/E, wafer world Inc.) and glass slides (VWR micro cover glass, 18x18mm), which served as flat substrates for MTMS films, were rinsed with acetone, methanol and isopropanol (BDH, ACS grade, 99%). Rinsed substrates were subsequently exposed to an air plasma for 5 minutes to remove any solvent residues and ensure the presence of hydroxyl groups on the surface. Cleaned substrates were immersed in the hydrolyzed MTMS solutions for 2 minutes. Control samples were also fabricated by immersing the cleaned substrates in pure, unhydrolyzed MTMS. After coating, excess liquid was removed from the surface by touching the liquid with a piece of tissue paper (Kimwipe, Kimberly-Clark). Coated substrates were then dried at ambient conditions overnight. A similar coating process was invoked for paper substrates. Handsheets with a size of 1.5 x 1.5 cm^2 were immersed in the hydrolyzed MTMS solutions for 2 minutes. To prevent over-coating, residual fluids were again removed after coating by using tissue paper. Coated paper was also dried under ambient conditions overnight before performing characterizations.

Contact angle measurements.

All static contact angle measurements were performed by using a Rame-Hart automated goniometer (model 290). A 4 µL droplet of the selected fluid (DI water, diiodomethane (Sigma-Aldrich, reagent plus grade, 99%), ethylene glycol (Sigma-Aldrich, anhydrous, 99.8%) and motor oil (SAE 10W-30, MotoTech)) was placed onto MTMS coated substrates. Contact angles were determined by the standard software of the goniometer (Drop Image, version 2.6.1).

SEM imaging.

All samples subjected to scanning electron microscopy (SEM) imaging were sputter coated with Au/Pd to reduce accumulation of charges during measurement. Images were taken with a Hitachi SU8230 SEM at an acceleration voltage of 5.0 keV.

Surface Analysis.

X-ray photoelectron spectroscopy (XPS) analyses were conducted using a Thermo Electron Corporation K-Alpha XPS system with a microfocused monochromatic Al Kα X-ray source. The spot size of the instrument is 400 µm.

FTIR analysis.

ATR-FTIR was carried out on a Nicolet IS-50 FTIR spectrometer (Thermo Scientific, Inc), operated in the ATR mode. The spectrometer was set to collect 32 scans at 4 cm^{-1} in the range from 4000 to 700 cm^{-1}.

NMR analysis.

^{29}Si NMR spectra were obtained for unhydrolyzed and hydrolyzed MTMS solutions on a Bruker Avance III 400 NMR spectrometer using a 5 mm broadband probe at 79.5 MHz. The ambient temperature (294K) was fixed during measurements. Deuterium oxide was used in lieu of DI water to prepare hydrolyzed samples. To obtain the control spectrum for unhydrolyzed MTMS, pure MTMS was mixed with methanol at a 4:1 ratio. Spectra were averaged over appropriate number of scans to enhance the signal-to-noise ratio. All chemical shifts were referenced to tetramethylsilane (TMS).

Air permeability analysis.

Air permeability of paper samples was determined following standard TAPPI T 460 om-02 procedure.[58] Samples with a size of 5 x 5 cm^2 were placed under a pressure differential of 1.22 kPa, and the time for 100 mL air to pass through paper was measured to determine the air permeability.

Profilometry.

Measurements were conducted using a Wyko NT3200 Optical Profilometer. Arithmetic averages of the surface roughness (i.e. Ra values) were analyzed using the Vision32 software (Veeco Instruments Inc.). Roughness was calculated according to the ANSI B46.1 standard.[59]

Results and discussion

Wetting properties of MTMS coated paper.

To investigate the effect of hydrolysis time on the wetting behavior of porous substrates, handsheets (HSs) were coated with MTMS hydrolyzed between 5 and 360 minutes. HSs are paper composed of only cellulose fiber, without chemical additives (e.g., fillers, brighteners). Compared to filter paper, for example, HSs are not designed to withstand prolonged exposure to fluids. Sonication was used during hydrolysis to enhance mixing and prevent gelation of MTMS at this high concentration; the process was conducted in an ice bath to remove heat generated by the exothermic hydrolysis reaction and maintain constant sample temperature. The mixture became less transparent after 30 minutes of hydrolysis, indicating formation of small particulates in the solution. After coating, treated HSs maintained the visual appearance of ordinary paper, including flexibility.

The wetting properties of coated HSs were determined through contact angle measurements (see Table 1). Water (surface tension 72.8 mN/m), diiodomethane (50.8 mN/m), ethylene glycol (48.0 mN/m) and motor oil (31.0 mN/m) were used as testing fluids that cover a wide range of fluid properties. Water and ethylene glycol are polar, while diiodomethane and motor oil are non-polar fluids. To evaluate the stability of oil contact angles, measurements were performed for 30 minutes after the droplet was placed on the substrate. For changes in contact angle less than 5°, the contact angle was considered to be stable; larger changes indicated an unstable contact angle. However, due to the relatively fast evaporation of water under ambient conditions, this method cannot be applied to evaluate the stability of the water contact angle. Instead, a dyed water droplet was placed on the coated paper, and its stability was evaluated by visually checking for signs of water absorption into the paper.

As shown in Table 1, both uncoated HSs and HSs coated with pure, unhydrolyzed MTMS absorb all fluids instantly. HSs coated with MTMS after 5 minutes of hydrolysis display a stable diiodomethane contact angle at 75° and a stable motor oil contact angle at 65°. However, the same sample absorbs water and ethylene glycol instantly. To our knowledge, this represents the first time that a hydrophilic/oleophobic surface has been fabricated on porous paper without the use of fluorinated materials. By further extending the hydrolysis time, the water repellency of coated HSs gradually increases, while oil contact angles remain essentially the same. HSs coated with MTMS after 60 minutes of hydrolysis still absorb water, but at a much slower rate, while HSs coated with MTMS after 180 minutes or 360 minutes of hydrolysis display stable water contact angles of ~90°. For ethylene glycol, on the other hand, all HS samples absorb the fluid, even at the longest hydrolysis time of 360 minutes. These results indicate that oleophobic paper with tunable hydrophilicity can be fabricated via a one-step coating process, using MTMS hydrolysis time as the controlling parameter. To explain this striking observation and determine the underlying mechanism, the chemistry of the MTMS solutions during the hydrolysis process and surface chemistry of the resulting coatings was investigated with various techniques, and the results of those studies are presented and discussed in the remainder of this paper.

MTMS hydrolysis process.

As shown above, MTMS hydrolysis time is a critical variable that greatly affects wetting properties, in particular for water. During hydrolysis, the stepwise substitutions of the alkoxide ligands by hydroxyl groups produce the reactive monomers that are subsequently consumed in condensation reactions to form dimers and oligomers. When hydrolyzed MTMS is coated on a substrate surface, those species form hydrogen bonds with the cellulose hydroxyl groups on the substrate. Finally, during drying, a permanent siloxane bond forms with concomitant loss of water. It is well-known that pH is an important parameter during the hydrolysis process; under acidic conditions, a fast hydrolysis reaction, followed by a slow condensation reaction, is observed.[60-63]

To examine the structural evolution of MTMS in both the early and late stages of hydrolysis, ^{29}Si NMR spectra were obtained for unhydrolyzed monomeric MTMS, and after 30 minutes and 180 minutes of hydrolysis (see Figure 1). Samples were scanned 256 times to ensure sufficient signal to noise ratio. Due to the long spin-lattice relaxation time of the silicon atoms, each spectrum took ~50 minutes to collect.

Table 1. Wetting behaviors of handsheets (HSs) coated with MTMS after different hydrolysis times.

MTMS Hydrolysis time (min)	Water	Ethylene glycol	Diiodomethane	Motor oil	Wetting behavior
Uncoated	Absorbs[a]	Absorbs	Absorbs	Absorbs	Hydrophilic/ Oleophilic
Pure MTMS	Absorbs	Absorbs	Absorbs	Absorbs	Hydrophilic/ Oleophilic
5	Absorbs	Absorbs	74.6±0.7°	64.7±1.4°	Hydrophilic/ Oleophobic
60	Unstable (77.4±3.4°)[b]	Absorbs	72.1±6.7°	64.4±2.1°	Hydrophilic/ Oleophobic
180	85.2±3.4°[c]	Absorbs	72.7±2.0°	61.2±2.5°	Amphiphobic
360	87.7±4.7°	Absorbs	68.1±4.1°	59.8±1.3°	Amphiphobic

[a] "Absorbs" indicates instant (<3 sec) absorption of the fluid. [b] "Unstable" indicates that the fluid is absorbed after some delay (>10 seconds); the number inside parentheses represents the contact angle immediately after the droplet was placed on these unstable samples. [c] Stable contact angles indicate that the change in contact angle is less than 5° within 30 minutes after drop placement.

Peak assignments were made according to literature.[39, 60, 61, 63] Signals with chemical shifts of -39.1 ppm, -47.6 pm, -57.2 ppm and -66.2 ppm can be assigned to MTMS monomer, dimer, linear oligomers and branched oligomers, respectively. Formation of cyclic species is also a common feature of MTMS hydrolysis under acidic conditions. Due to reduction of the Si-O-Si angle, these peaks are located further downfield relative to linear and branched species:[61] peaks at -56.5 ppm and -64.3 ppm are assigned to 4- membered ring and caged species, respectively. The disappearance of monomeric MTMS species after 30 minutes of hydrolysis indicates a fast process. In comparison, condensation is relatively slow in the presence of acid. All forms of condensed species (dimers, linear oligomers and branched oligomers) are observed in MTMS hydrolyzed for 30 minutes. As the reaction continues, condensation becomes dominant. As a result, the signal from MTMS dimers disappears and more branched and caged oligomers are observed after 180 minutes. Because MTMS dimers and linear oligomers contain more silanol groups than branched oligomers, when coated on substrates, MTMS hydrolyzed for shorter periods of time is expected to display more polar silanol groups on the surface than MTMS with a prolonged hydrolysis. To test the validity of this hypothesis, the surface chemistry of MTMS coatings with different hydrolysis times was carefully characterized using XPS and ATR-FTIR.

Surface chemistry of MTMS coatings.

To investigate changes in surface composition as a function of hydrolysis time, XPS was performed on silicon wafers coated with MTMS. A silicon wafer was chosen as the substrate for this study because it has a well-defined, flat surface. The effects of surface roughness on wetting behavior can therefore be excluded. A clean silicon wafer without MTMS coating was used as a control sample. As expected, carbon, oxygen and silicon were the only three elements detected on all samples (see supplementary Figure S1).

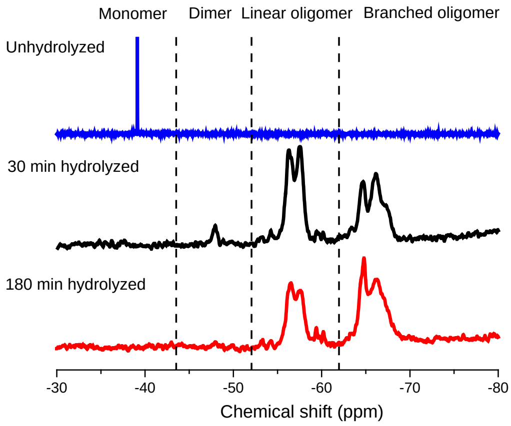

Figure 1. ^{29}Si NMR spectra after different hydrolysis times for acid catalyzed MTMS.

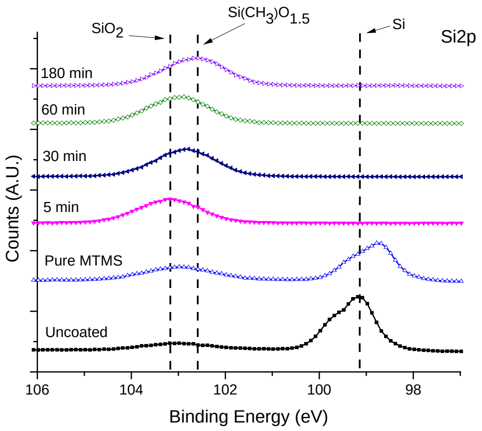

Figure 2. XPS data for Si 2p on silicon wafers coated with MTMS after different hydrolysis times. Peaks in the 95-110 eV range correspond to the $2p^{1/2}$ and $2p^{3/2}$ peaks of Si.

To further investigate changes in surface chemistry with hydrolysis time, high resolution XPS spectra were also taken. Figure 2 presents XPS spectral scans for MTMS films on silicon for different hydrolysis times. Before coating, Si (99.4 eV) and SiO_2 (103.2 eV) are present on the surface; these two peaks are preserved on the surface of the sample coated with unhydrolyzed MTMS, indicating that pure, unhydrolyzed MTMS cannot form a continuous thin film on silicon within 2 minutes, which can be attributed to the fact that pure MTMS lacks silanol groups to form covalent bonds with Si-OH on the substrate surface. After 5 minutes of hydrolysis, the elemental Si peak has disappeared, which is strong evidence that the surface is fully covered by condensed MTMS species. A closer inspection of the XPS spectra reveals that as hydrolysis time increases further, peaks around 103 eV gradually shift towards a lower binding energy. This gradual shift is likely due to a change in MTMS species from dimers to linear polymers and branched polymers, as the condensation reaction progresses. The peak shift between the 5 and 30 minute samples also indicates that the hydrolysis reaction predominantly occurs during the sonication step and that the reactivity during the subsequent coating and drying steps is much lower. After 180 minutes of hydrolysis, this peak is finally shifted to 102.8 eV, which corresponds to fully cross-linked $Si(CH3)O_{3/2}$ species, according to literature.[64]. However, because of the subtle difference in XPS spectra between O-Si-O-H and O-Si-O-Si signatures,[65] it is very difficult to extract quantitative information from this peak shift.

To further investigate the surface chemistry on different MTMS films, ATR-FTIR spectra were taken on uncoated glass slides and glass slides coated with MTMS hydrolyzed from 0 to 360 minutes (Figure 3a). Glass slides were used as substrates in this set of experiments in lieu of silicon wafers to avoid overlap with broad Si-O-Si IR peaks from the underlying substrate.

It is evident from Figure 3a that the spectrum for pure MTMS is similar to that of the uncoated substrate, which further confirms that unhydrolyzed MTMS cannot graft onto glass slides during a short coating time. The spectrum for the glass slide coated with 5 minutes hydrolyzed MTMS shows strong peaks at 1100 cm^{-1}, which correspond to Si-O-Si bonds,[66] indicating that MTMS has been successfully grafted onto the substrate surface following a short hydrolysis time. The peaks at 1270 cm^{-1} and 760 cm^{-1} can both be assigned to $Si-CH_3$ bonding.[67] The presence of methyl groups on the surface is further confirmed by the peak at 2950 cm^{-1}, which is due to C-H bonding. However, due to the relatively short hydrolysis time, large amounts of MTMS dimers and linear oligomers are still present in the mixture. Both of these species contain silanol groups, resulting in peaks at 890 cm^{-1} and 3300 cm^{-1} from Si-OH and O-H bonding, respectively. The presence of both methyl groups and hydroxyl groups on the substrate surface is the primary reason for the unique wetting properties of MTMS coated substrates, which is discussed in more details below. As the hydrolysis time increases, MTMS dimers and linear polymers further react through condensation reactions and form branched oligomers. Consequently, peaks at 890 cm^{-1} and 3300 cm^{-1} gradually reduce in intensity, while the peaks corresponding to Si-O-Si and $Si-CH_3$ are preserved after prolonged hydrolysis. This result clearly proves that the concentration of hydroxyl groups on the substrate surface can be controlled by changing hydrolysis time of MTMS in an acidic environment. MTMS solutions with short hydrolysis time contain more dimers and linear oligomers, and are therefore rich in hydroxyl groups. As the condensation reaction continues, more branched oligomers are generated in the MTMS solution; as a result, hydroxyl groups on the substrate surface also gradually disappear. In addition to the glass slides, the surface chemistry of uncoated and coated HSs was also characterized using ATR-FTIR (see Figure 3b). Although the spectra on the chemically more heterogeneous HS are more difficult to interpret, the data in Figure 3a greatly assist with peak assignment and analysis. It is clear that HSs coated with pure MTMS display a similar spectrum to that of the uncoated HS, again confirming the low surface reactivity of unhydrolyzed MTMS. Peaks corresponding to the $Si-CH_3$ bond (1270 cm^{-1}, 760 cm^{-1}) and methyl group (2950 cm^{-1}) are evident in the spectrum for HSs coated after 5 minutes or 180 minutes of MTMS hydrolysis. This result indicates that despite the rough surface of the porous HS, MTMS can successfully graft to hydroxyl groups on the HS surface following a short hydrolysis time. However, due to the large number of hydroxyl groups on native cellulose fibers, all samples display peaks at 3300 cm^{-1}. As a result, unlike the glass substrates, the density of hydroxyl groups on different HS samples cannot be directly compared based on ATR-FTIR.

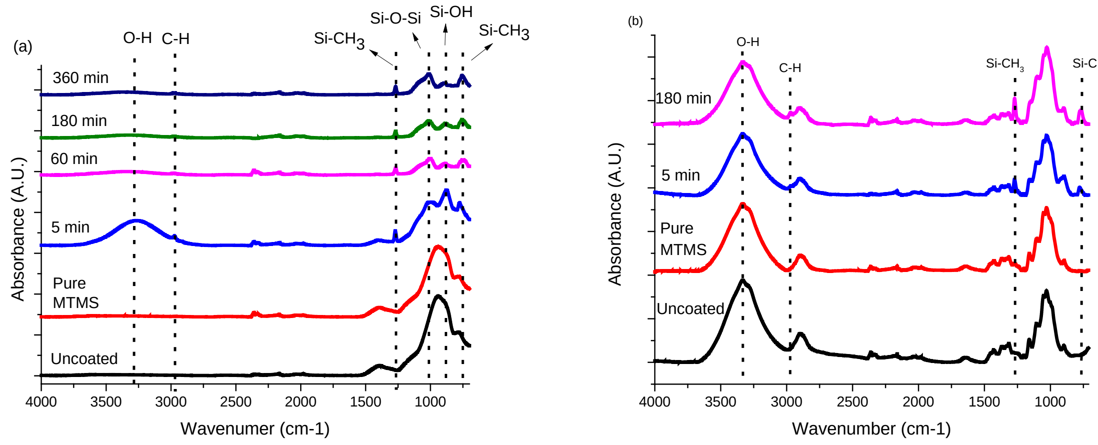

Figure 3. ATR-FTIR of (a) MTMS coated glass slides and (b) MTMS coated HSs after different MTMS hydrolysis times.

Wetting properties of MTMS films.

Both surface chemistry and surface morphology can affect the wetting properties. To isolate the effects of surface chemistry, contact angles (CA) were measured on silicon wafers coated with MTMS after different hydrolysis times. The wetting behavior of MTMS films is summarized in Figure 4. Before coating, cleaned silicon wafers have a diiodomethane CA of 40.4°± 0.6° and a motor oil CA of 20.1°±2.3°. For silicon wafers coated with pure MTMS, an increase in both diiodomethane and motor oil contact angles was observed. According to our NMR and FTIR data, this phenomenon is likely due to small amounts of unhydrolyzed MTMS monomer physisorbed onto the substrate. The introduction of methyl groups imparts oleophobicity to the surface due to their low surface energy.[37] For wafers coated with 5 minutes hydrolyzed MTMS, the diiodomethane and –most notably- motor oil contact angles increase further. Based on our previous ATR-FTIR observations, this result is due to the presence of a high concentration of methyl groups grafted to the substrate. Further increasing the hydrolysis time has little effect on the contact angles of non-polar fluids, indicating that the density of methyl groups on the surface does not change significantly with prolonged hydrolysis time.

Compared to non-polar fluids, water shows a very different wetting behavior as a function of MTMS hydrolysis time. The stability of the water contact angle was evaluated by observing the spreading dynamics of water droplets during the contact angle measurements. On the uncoated silicon wafer, due to the high density of hydroxyl groups on the surface, water wets the surface completely in less than 5 seconds (i.e. zero degree contact angle). For silicon wafers coated with pure MTMS, a stable water contact angle of 58.5° was observed, again indicating the presence of physisorbed unhydrolyzed MTMS. However, complete wetting was observed on silicon wafers coated with MTMS hydrolyzed for 5 minutes. Because less than 5 seconds elapsed before water completely spread on the surface, a 0° water contact angle is reported here. It should be pointed out that for other, fluorinated hydrophilic/oleophobic materials, it usually requires minutes before water contact angles drop to less than 20°, while in our case water wets the coated surface almost immediately.[33, 68, 69] Our NMR and ATR-FTIR results suggest that the hydrophilic behavior of the substrate coated with MTMS after a short hydrolysis time is due to the abundance of polar hydroxyl groups in hydrolyzed, but not fully condensed MTMS dimers or linear oligomers in the mixture. When coated on a silicon wafer, both methyl groups and hydroxyl groups are present on the substrate surface, as indicated by ATR-FTIR spectra. The contact angle of non-polar fluids is largely determined by the density of non-polar methyl groups on the substrate surface. On the other hand, water is very sensitive to the presence of hydroxyl groups. As our previous analysis indicates, as hydrolysis time increases, the condensation reaction becomes dominant, and the concentration of silanol groups slowly decreases. Indeed, for substrates coated with MTMS after 60 minutes hydrolysis, a much slower water wetting behavior was observed. For MTMS hydrolyzed for more than 180 minutes, stable water contact angles were found. As summarized in Figure 4, by tuning hydrolysis time, MTMS coated surfaces can be fabricated on a non-porous substrate with controlled wetting behavior against water but these surfaces maintain similar oil contact angles.

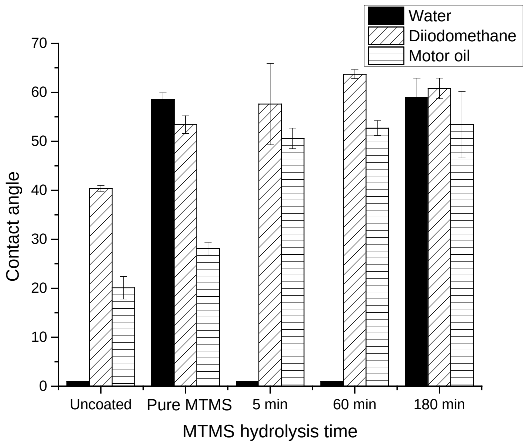

Figure 4. Contact angle measurement of water, diiodomethane and motor oil on silicon wafers coated with MTMS after different hydrolysis times.

To further illustrate the point that wetting on a MTMS coated substrate is not solely determined by surface energy, but also highly dependent on the polarity of fluids, ethylene glycol contact angles were measured on different samples. Ethylene glycol has a surface tension similar to that of diiodomethane, but it displays a completely different wetting behavior on MTMS coated silicon wafers. As is evident in Figure 5, ethylene glycol displays a wetting behavior that is similar to water. Because ethylene glycol has a much lower vapor pressure than water, it is possible to monitor changes in contact angle for 30 minutes without evaporation effects. An uncoated silicon wafer displays a 0° ethylene glycol contact angle. A stable ethylene glycol contact angle of 46° is observed on silicon wafers coated with pure MTMS. The contact angle is lower than that of water because ethylene glycol has a lower surface tension. For silicon wafers coated with hydrolyzed MTMS, a similar trend was observed as that for water: with an increase in hydrolysis time, the resistance against wetting also increases.

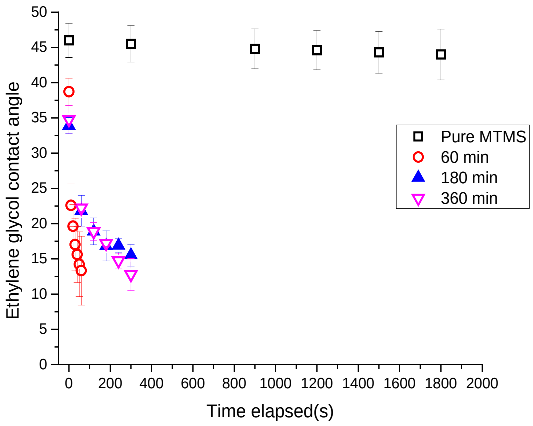

Figure 5. Contact angle measurements of ethylene glycol on silicon wafers coated with MTMS hydrolyzed for different times as a function of elapsed time after droplet placement.

The main difference between water and ethylene glycol is that due to the lower surface tension of ethylene glycol, all samples display a lower wetting resistance against ethylene glycol than water; even after 360 minutes of hydrolysis, ethylene glycol spreads on the surface within 5 minutes.

Properties of MTMS coated paper.

Based on the wetting properties and surface chemistry of MTMS thin films on flat substrates, the remarkable wetting properties of MTMS-coated paper HSs (Table 1) can now be explained. On a porous substrate, pure MTMS cannot form a coating that is sufficiently dense to support non-polar fluids; as a result, both uncoated HSs and HSs coated with pure MTMS display oleophilicity. The increased density of methyl groups after 5 minutes of hydrolysis imparts oil resistance to the paper. Similar to the wetting behavior of MTMS films on flat substrates, a further increase in hydrolysis time has no significant effect on oil contact angles. To determine if coated HSs can display prolonged oil resistance, a droplet of motor oil, which has a much lower surface tension than diiodomethane, was monitored over 12 hours (see Figure 6a). No oil stains were observed on the paper after 12 hours and the change in contact angle was less than 5°. In fact, we have observed that droplets of motor oil can remain on HSs coated with hydrolyzed MTMS for several weeks without any signs of absorption.

The wetting behavior of polar fluids on MTMS coated HSs is also similar to silicon wafers (see Figure 6b). The hydrophilicity of HSs coated with pure MTMS is likely due to low grafting density. Due to the high concentration of hydroxyl groups, HSs coated with MTMS after 5 minutes hydrolysis absorbed water instantly. As the hydrolysis time increases, the concentration of silanol groups decreases. Consequently, HSs coated by MTMS after a prolonged hydrolysis time display higher resistance toward water. Analogous to the wetting properties of MTMS films on flat silicon wafers, none of the coated HS samples show resistance towards ethylene glycol wetting. In fact, all coated HSs absorb ethylene glycol at a much faster rate than its spreading rate on MTMS coated wafers.

To test the thermal stability of hydrophilic-oleophobic paper, HSs coated with 5 minute and 180 minute hydrolysed MTMS were heated at 120°C for 15 minutes. These heat-treated samples exhibited the same wetting behavior as unheated samples, indicating good thermal stability. However, it has been reported previously that silanol groups may react with each other at high temperature and it is possible that the unique wetting behavior of our MTMS coated paper will be compromised after prolonged heating that may occur during applications under more extreme conditions.[70]

In previous studies, liquid-repellent paper was fabricated by applying a pore-free barrier coating on top of the fiber surface.[35, 71-75] The obvious disadvantage of this approach is the loss of intrinsic flexibility and air permeability. In the current study, overcoating was prevented by reducing the coating time to 2 minutes and removing excessive MTMS immediately after coating. To study the morphology of coated

HSs, SEM and optical profilometry were used to characterize different samples (see Figure 7). At low magnification, the SEM images do not reveal a significant difference between coated and uncoated HSs: the porosity of uncoated paper is largely retained for MTMS coated HS. However, at high magnification, a thin coating layer can clearly be seen around each individual fiber for MTMS coated HSs. To study the topology before and after coating in more detail, roughness profiles were measured with an optical profilometer. Again, the difference between uncoated and coated HSs appears to be minimal, and all samples show similar micron-scale roughness. To further confirm the retention of sample porosity after coating, a droplet of dyed methanol was placed on each sample. With its much lower surface tension (22.5 mN/m), methanol immediately penetrated through all treated papers, leaving stains on paper substrates placed beneath the test paper, thus confirming that no continuous film has been formed on the coated paper surface.

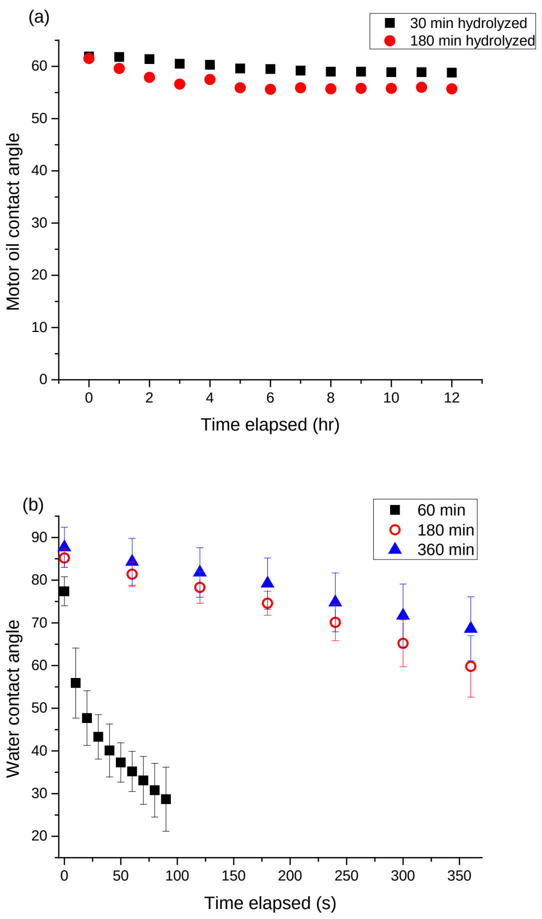

Figure 6. Contact angle measurements of (a) motor oil and (b) water on HSs coated with MTMS hydrolyzed for different times as a function of elapsed time.

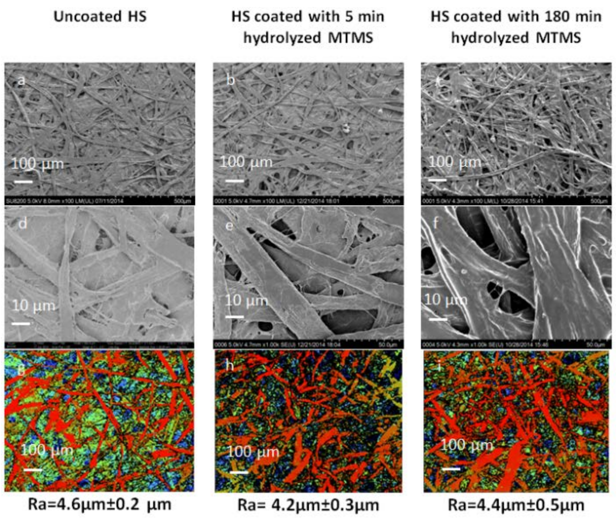

Figure 7. Low magnification SEM images of uncoated HSs, HSs coated with 5 min hydrolyzed MTMS and HSs coated with 180 min hydrolyzed MTMS are shown in (a-c), demonstrating that the porosity of native paper is largely retained after coating. Complementary high magnification SEM images are presented in (d-f). Profilometer images for each sample are also presented in (g-i)

To quantitatively determine any changes in air permeability after coating, Gurley air permeability tests were conducted according to TAPPI T-460 procedure on MTMS coated paper (see Table 2). The Gurley air permeability test is a common method used in the paper industry to evaluate air permeability of coated paper; it measures the time for 100 mL of air to pass through the paper under a pressure differential of 1.22 kPa. A decrease in air permeability was observed for samples coated with hydrolyzed MTMS, likely because the MTMS coatings partly cover small pores in the fibrous network, resulting in lower porosity. However, it should be noted that a factor 6 increase in flow time is actually quite low compared to other fluid-repellent paper substrates with barrier coatings, which typically show decreased air permeability by factors of 100 to 10,000.[71] In our samples, the majority of pores are clearly retained after the coating process.

Table 2. Air permeability of HS coated with MTMS after different times

MTMS hydrolysis time (min)	Permeability (s)
Uncoated	25.8±1.0
0	23.9±1.0
5	120.7±2.4
60	131.7±1.8
180	144.7±1.0

Conclusions

We have developed a facile, one-step solution coating method to fabricate oleophobic paper substrates with tunable hydrophilicity using non-fluorinated coating material. The coating material was easily prepared by mixing pure methyltrimethoxysilane (MTMS) with 0.1 M hydrochloric acid at a 4:1 ratio, followed by sonication in an ice bath. The hydrophilicity of MTMS coatings can be tuned by simply adjusting hydrolysis time. Consequently, coated surfaces display wetting behaviors ranging from hydrophilic/ oleophobic to amphiphobic as a function of hydrolysis time.

Compared with existing hydrophilic/ oleophobic surfaces, which are commonly fabricated on well-defined, flat substrates, MTMS coatings can easily be applied on more heterogeneous, porous substrates such as paper. Moreover, this material does not contain fluorine and is therefore more environmental friendly than those previously reported. The porous structure of paper is also largely retained after coating, which improves flexibility and air permeability relative to that of other grease-proof papers. The MTMS coating process is carried out in an aqueous environment under ambient conditions at a relatively fast rate. As a result, it is compatible with current large-scale paper manufacturing processes. Development of hydrophilic/oleophobic paper surfaces will facilitate important applications such as oil/water separation; further studies are underway to explore this in more detail. The amphiphobic paper has potential applications as packaging materials that can repel both aqueous and oily fluids, as a self-cleaning material, and as a material for disposable labware. This work also indicates that MTMS can be employed to functionalize other hydroxyl-group-rich surfaces.

Acknowledgements

The authors thank the Renewable Bioproducts Institute (RBI) at the Georgia Institute of Technology and SAPPI Fine Paper North America for funding support of Z. Tang. The authors also thank SAPPI Fine Paper North America for generously donating the pulp. Z. Tang also thanks Dr. Amy Blakeley and Dr. Lester Li (SAPPI Fine Paper North America) for helpful suggestions.

Notes and References

1. A. C. Zettlemoyer, *J. Colloid Interface Sci.*, 1968, **28**, 343.
2. J. Sagiv, *J. Am. Chem. Soc.*, 1980, **102**, 92.
3. A. Raghavanpillai, S. Reinartz and K. W. Hutchenson, *J. Fluorine Chem.*, 2009, **130**, 410.
4. G. J. Kahan, *J. Colloid Interface Sci.*, 1951, **6**, 571.
5. L. Gao and T. J. McCarthy, *J. Am. Chem. Soc.*, 2006, **128**, 9052.
6. L. Feng, S. H. Li, Y. S. Li, H. J. Li, L. J. Zhang, J. Zhai, Y. L. Song, B. Q. Liu, L. Jiang and D. B. Zhu, *Adv. Mater.*, 2002, **14**, 1857.
7. F. Dong and C.-S. Ha, *Macromol. Res.*, 2011, **19**, 101.
8. C. Aulin, S. H. Yun, L. Wagberg and T. Lindstrom, *ACS Appl. Mater. Interfaces*, 2009, **1**, 2443.
9. J. Yang, Z. Z. Zhang, X. H. Xu, X. T. Zhu, X. H. Men and X. Y. Zhou, *J. Mater. Chem.*, 2012, **22**, 2834.
10. J. A. Howarter and J. P. Youngblood, *Adv. Mater.*, 2007, **19**, 3838.
11. J. A. Howarter and J. P. Youngblood, *Macromol. Rapid Commun.*, 2008, **29**, 455.
12. A. B. D. Cassie and S. Baxter, *Trans. Faraday Soc.*, 1944, **40**, 546.
13. A. Marmur, *Langmuir*, 2003, **19**, 8343.
14. B. Wang, J. Li, G. Wang, W. Liang, Y. Zhang, L. Shi, Z. Guo and W. Liu, *ACS Appl. Mater. Interfaces*, 2013, **5**, 1827.
15. N. Verplanck, E. Galopin, J.-C. Camart, V. Thomy, Y. Coffinier and R. Boukherroub, *Nano Lett.*, 2007, **7**, 813.
16. J. G. Nguyen and S. M. Cohen, *J. Am. Chem. Soc.*, 2010, **132**, 4560.
17. S. Li, S. Zhang and X. Wang, *Langmuir*, 2008, **24**, 5585.
18. C. Dorrer and J. Ruehe, *Adv. Mater.*, 2008, **20**, 159.
19. B. Balu, V. Breedveld and D. W. Hess, *Langmuir*, 2008, **24**, 4785.
20. S. Amigoni, E. T. de Givenchy, M. Dufay and F. Guittard, *Langmuir*, 2009, **25**, 11073.
21. S. Pan, R. Guo and W. Xu, *Soft Matter*, 2014, **10**, 9187.
22. J. Zhang and S. Seeger, *Angew. Chem., Int. Ed.*, 2011, **50**, 6652.
23. B. Leng, Z. Shao, G. de With and W. Ming, *Langmuir*, 2009, **25**, 2456.
24. A. Tuteja, W. Choi, M. Ma, J. M. Mabry, S. A. Mazzella, G. C. Rutledge, G. H. McKinley and R. E. Cohen, *Science*, 2007, **318**, 1618.
25. L. Li, V. Breedveld and D. W. Hess, *ACS Appl. Mater. Interfaces*, 2013, **5**, 5381.
26. H. Zhou, H. X. Wang, H. T. Niu and T. Lin, *Sci. Rep.*, 2013, **3**, 1.
27. R. Molina, M. Gomez, C. W. Kan and E. Bertran, *Cellulose*, 2014, **21**, 729.
28. K. S. Liu, Y. Tian and L. Jiang, *Prog. Mater Sci.*, 2013, **58**, 503.
29. R. A. Lampitt, J. M. Crowther and J. P. S. Badyal, *J. Phys. Chem. B*, 2000, **104**, 10329.
30. S. J. Hutton, J. M. Crowther and J. P. S. Badyal, *Chem. Mater.*, 2000, **12**, 2282.
31. J. A. Howarter and J. P. Youngblood, *J. Colloid Interface Sci.*, 2009, **329**, 127.
32. J. A. Howarter, K. L. Genson and J. P. Youngblood, *ACS Appl. Mater. Interfaces*, 2011, **3**, 2022.
33. H. Sawada, Y. Ikematsu, T. Kawase and Y. Hayakawa, *Langmuir*, 1996, **12**, 3529.
34. A. K. Kota, G. Kwon, W. Choi, J. M. Mabry and A. Tuteja, *Nature Communications*, 2012, **3**, 1.
35. K. Rohrbach, Y. Y. Li, H. L. Zhu, Z. Liu, J. Q. Dai, J. L. Andreasen and L. B. Hu, *Chem. Commun.*, 2014, **50**, 13296.
36. P. S. Brown, O. Atkinson and J. P. S. Badyal, *ACS Appl. Mater. Interfaces*, 2014, **6**, 7504.
37. E. G. Shafrin and W. A. Zisman, *J. Phys. Chem.*, 1960, **64**, 519.
38. A. Siriviriyanun and T. Imae, *Chem. Eng. J.*, 2014, **246**, 254.
39. Z. Zhang, G. Sebe, D. Rentsch, T. Zimmermann and P. Tingaut, *Chem. Mater.*, 2014, **26**, 2659.
40. M. A. Tshabalala, P. Kingshott, M. R. VanLandingham and D. Plackett, *J. Appl. Polym. Sci.*, 2003, **88**, 2828.
41. H. Miyafuji and S. Saka, *Mater. Sci. Res. Int.*, 1999, **5**, 270.

42. P. Hochmanska, B. Mazela and T. Krystofiak, *Drewno*, 2014, **57**, 99.
43. M. M. Kulkarni, R. Bandyopadhyaya and A. Sharma, *J. Mater. Chem.*, 2008, **18**, 1021.
44. K. O. Jang and K. Yeh, *Text. Res. J.*, 1993, **63**, 557.
45. T. Fei, H. Chen and J. Lin, *Colloids and Surfaces, A: Physicochemical and Engineering Aspects*, 2014, **443**, 255.
46. J. T. Wang, Y. A. Zheng and A. Q. Wang, *Chem. Eng. J.*, 2012, **213**, 1.
47. S. H. Li, S. B. Zhang and X. H. Wang, *Langmuir*, 2008, **24**, 5585.
48. F. Girardi, S. Maggini, C. Della Volpe, E. Cappelletto, K. Mueller, S. Siboni and R. Di Maggio, *J. Sol-Gel Sci. Technol.*, 2011, **60**, 315.
49. O. Yagi, Y. Iwamiya, K. Suzuki, R. Funane and F. Ohishi, *J. Sol-Gel Sci. Technol.*, 2005, **36**, 69.
50. J. Y. Wang, M. R. N. Monton, X. Zhang, C. D. M. Filipe, R. Pelton and J. D. Brennan, *Lab Chip*, 2014, **14**, 691.
51. J. Yang, H. J. Song, X. H. Yan, H. Tang and C. S. Li, *Cellulose*, 2014, **21**, 1851.
52. P. Ragesh, V. A. Ganesh, S. V. Naira and A. S. Nair, *J. Mater. Chem. A*, 2014, **2**, 14773.
53. X. Y. Zhu, W. T. Tu, K. H. Wee and R. B. Bai, *J. Membr. Sci.*, 2014, **466**, 36.
54. D. Graiver, K. W. Farminer and R. Narayan, *J. Polym. Environ.*, 2003, **11**, 129.
55. V. K. Rowe, H. C. Spencer and S. L. Bass, *J. Ind. Hyg. Toxicol.*, 1948, **30**, 332.
56. G. Ciapetti, D. Granchi, S. Stea, L. Savarino, E. Verri, A. Gori, F. Savioli and L. Montanaro, *J. Biomed. Mater. Res.*, 1998, **42**, 485.
57. TAPPI, *Forming handsheets for physical tests of pulp*, Technical Association of Paper and Pulp Industry, Atlanta, GA, 2002.
58. TAPPI, *Air resistance of paper (Gurley method)*, Technical Association of Paper and Pulp Industry, Atlanta, GA, 2006.
59. ANSI, *Surface Texture (Surface Roughness, Waviness, and Lay)*, Americal National Standard Institution, Washington, DC, 1995.
60. T. M. Alam, R. A. Assink and D. A. Loy, *Chem. Mater.*, 1996, **8**, 2366.
61. H. J. Dong, M. Lee, R. D. Thomas, Z. P. Zhang, R. F. Reidy and D. W. Mueller, *J. Sol-Gel Sci. Technol.*, 2003, **28**, 5.
62. Z. P. Zhang, B. P. Gorman, H. J. Dong, R. A. Orozco-Teran, D. W. Mueller and R. F. Reidy, *J. Sol-Gel Sci. Technol.*, 2003, **28**, 159.
63. H. J. Dong, Z. P. Zhang, M. H. Lee, D. W. Mueller and R. F. Reidy, *J. Sol-Gel Sci. Technol.*, 2007, **41**, 11.
64. M. R. Alexander, R. D. Short, F. R. Jones, W. Michaeli and C. J. Blomfield, *Appl. Surf. Sci.*, 1999, **137**, 179.
65. L. A. O'Hare, B. Parbhoo and S. R. Leadley, *Surf. Interface Anal.*, 2004, **36**, 1427.
66. A. V. Rao, M. M. Kulkarni, D. P. Amalnerkar and T. Seth, *J. Non-Cryst. Solids*, 2003, **330**, 187.
67. P. J. Launer, *Silicon Compounds: Silanes & Silicones*, Gelest, Inc, Morrisville, PA, 2013.
68. H. Sawada, H. Yoshioka, T. Kawase, H. Takahashi, A. Abe and R. Ohashi, *J. Appl. Polym. Sci.*, 2005, **98**, 169.
69. D. Tian, X. Zhang, Y. Tian, Y. Wu, X. Wang, J. Zhai and L. Jiang, *J. Mater. Chem.*, 2012, **22**, 19652.
70. S. J. Pan, R. Guo and W. J. Xu, *AIChE J.*, 2014, **60**, 2752.
71. C. Aulin, M. Gallstedt and T. Lindstrom, *Cellulose*, 2010, **17**, 559.
72. N. Lavoine, I. Desloges, A. Dufresne and J. Bras, *Carbohydr. Polym.*, 2012, **90**, 735.
73. J. Han, S. Salmieri, C. Le Tien and M. Lacroix, *J. Agric. Food. Chem.*, 2010, **58**, 3125.
74. M. Havimo, J. Jalomaki, M. Granstrom, A. Rissanen, T. Iivanainen, M. Kemell, M. Heikkila, M. Sipi and I. Kilpelainen, *Packag. Technol. Sci.*, 2011, **24**, 249.
75. S. Paunonen, *Nord. Pulp Pap. Res. J.*, 2013, **28**, 165.

Graphical Abstract/ToC

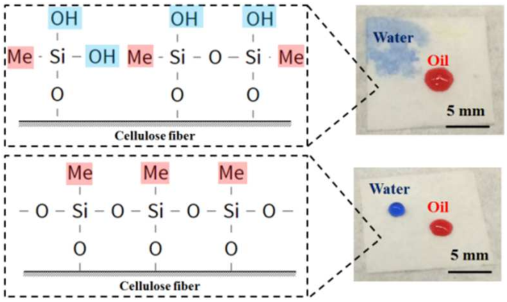

Oleophobic paper with tunable hydrophilicity is fabricated by varying the concentration of polar groups using non-fluorinated coating materials.